Digital Camera Technologies for Scientific Bio-Imaging. Part 2: Sampling and Signal

Yashvinder Sabharwal, [1] *James Joubert* [2] *and Deepak Sharma* [2]
1. Solexis Advisors LLC, Austin, TX, USA 2. Photometrics and QImaging, Tucson, AZ, USA

ABSTRACT
This article develops a methodology for understanding the balance between imaging and radiometric properties in microscopy systems where digital sensors (CCD, EMCCD, and scientific-grade CMOS) are utilized. The methodology demonstrates why smaller pixel cameras provide better sampling at low magnifications and why these cameras are less efficient at collecting light than medium and larger pixel cameras. The article also explores how different optical configurations can improve light throughput while maintaining adequate sampling with smaller pixel cameras.

AUTHOR DETAILS
Yashvinder Sabharwal, Solexis Advisors LLC, 6103 Cherrylawn Circle, Austin, TX 78723, USA
Mob: +1 512 534 8340
Email: yash@solexis-advisors.com
James Joubert, Applications Scientist, Photometrics and QImaging
3440 East Britannia Drive
Tucson, AZ 85706-5006, USA
Tel: +1 520 889 9933
Email jjoubert@photometrics.com

INTRODUCTION

CCD and EMCCD technologies have become the standard in bio-imaging over the years and each has been well characterized in numerous applications. More recently, the scientific-grade CMOS has been developed for scientific bio-imaging and is finding its way into different bio-imaging applications. CMOS technology has had issues in the past, but recent improvements indicate room for its use within the array of current imaging applications. This four-part series aims to compare these major camera technologies and discuss a methodology for selecting the appropriate sensor technology for a given application.

Part 1 of this series [1] introduced the different camera technologies, describing how they function and some of the key differences between them. In Part 2, we now look to compare the performance of typical CCD, EMCCD, and CMOS sensors evaluating both imaging parameters *and* radiometric (light throughput) parameters. Although comparative in nature, the purpose of this article and this series is not to state that one technology is better than the others across the spectrum of bio-imaging applications, but rather to discuss the critical optical parameters which should be considered when selecting a camera for a particular application.

This article attempts to simplify the analysis by first separating the metrics into imaging/sampling and radiometric, i.e. light throughput, considerations. The discussion begins by introducing the detection arm of a fluorescence imaging system and evaluating the standard pixel sizes of the three sensor technologies with respect to resolution and sampling. Complementing this analysis is a discussion of the methodology for calculating the number of photons that will be incident at

each pixel of the sensor. Real experimental parameters, such as dye concentration, numerical aperture (NA), and magnification, are all considered to determine this photon throughput.

In Parts 3 and 4 of the series, the analysis of radiometric throughput will be combined with an analysis of system noise to generate signal-to-noise profiles as a function of exposure time to help select which sensor would be best for a particular application.

Detection Arm
Any fluorescence imaging system which excites a sample at one wavelength and detects emission at another longer wavelength will be comprised of an illumination arm and detection arm. In many instances, both optical arms will share some optical components, such as the objective lens in an epi-fluorescence imaging system. The optical parameters of the illumination arm affect the amount of excitation light incident on the sample and the optical parameters of the detection arm will affect imaging resolution and the final signal-to-noise ratio of the detected image.

Figure 1 shows a schematic of an epi-fluorescence microscope optical configuration. The illumination beam (blue) is reflected by the dichroic filter toward the objective lens and emerges from the objective lens to excite the sample. In this example, the objective lens is telecentric in the sample space which means that the magnification of the object will stay relatively constant with defocus. The sample, which has been excited by optical illumination, emits light (red) which is collected by the objective lens, filtered in collimated space with a bandpass filter, and re-imaged onto a sensor using a tube lens. Clearly, the objective lens is
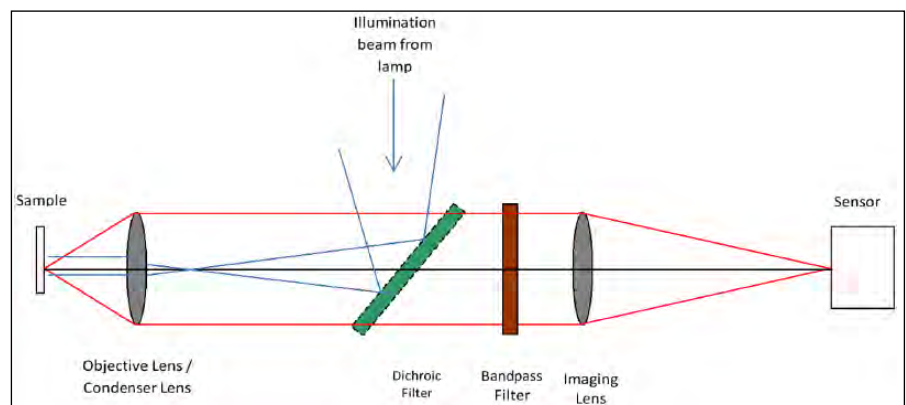

Figure 1:
Schematic of the optical configuration of an epi-fluorescence microscope.

the most important element in this analysis and the critical parameters are the numerical aperture (NA) of the objective lens and the magnification (M) of objective lens.

IMAGING ANALYSIS

Spatial Resolution and Sampling
The primary metric of concern in epi-illumination imaging systems is the lateral resolution. Lateral resolution refers to the resolution in the plane of the sample being imaged. As the value of the resolution parameter decreases, smaller features can be resolved by the imaging system. In an epi-illumination system, lateral resolution at the sample is a function of two parameters, the wavelength λ of the emitted light and the NA of the objective lens. Since the NA incorporates the index of refraction of the immersion medium of the objective lens, we do not have to consider this variable separately. The most familiar resolution limits are the Abbe limit (R_a) and the Rayleigh limit (R_r) [2]. Both of these resolution limits are based on optical diffraction theory, and they differ slightly in their proportionality constant. These limits assume that the detection arm imaging system is free of aberrations. While we know this not to be true, it provides a lower limit, and it does simplify the calculations for this analysis:

$$\text{At object} \rightarrow R_a = 0.5\,\lambda\,/\,NA \qquad (1)$$

$$\text{At object} \rightarrow R_r = 0.61\,\lambda\,/\,NA \qquad (2)$$

If these resolution limits are multiplied by the magnification (M) of the objective, one can calculate the minimum resolvable feature size at the location of the image where the CCD, EMCCD, or scientific-grade CMOS sensor is placed. Equation 3 shows the resolution at the detector R_d using the Rayleigh limit:

$$\text{At detector} \rightarrow R_d = 0.61\,M\,\lambda\,/\,NA \quad (3)$$

Figure 2 provides a graphical representation of the resolution limit, in this case the Rayleigh limit, where two adjacent spots are imaged as two Airy disks (due to diffraction) and are resolved when the center of one Airy disk overlaps the first minimum of the adjacent Airy disk.

Any image sensing technology, whether it is a CCD or film or your eye, is comprised of discrete imaging elements. In the case of CCDs, you have pixels; with film you have grains of silver halide; and your eye has rods and cones. When an image is recorded using a discrete imaging system, the image is automatically sampled. If the parameters of the discrete imaging system are not properly matched to the resolution limit of your imaging system, you can introduce errors into the sampled image known as aliasing. Aliasing leads to errors in intensity distribution, so care must be taken to ensure the validity of any quantitative conclusions being drawn from images not correctly sampled. An example of an aliasing artifact is shown in Figure 3.
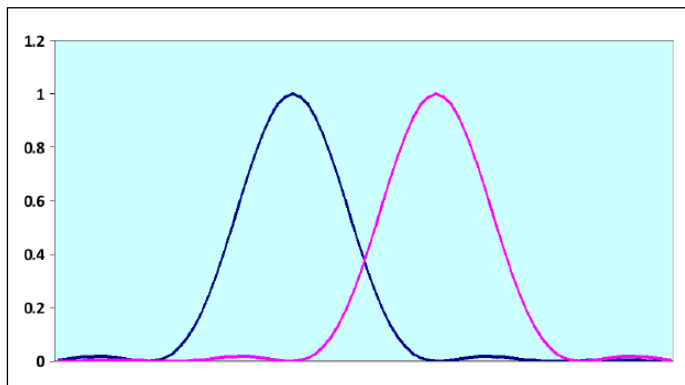
Figure 4 shows the combined intensity pro-

file of the two Airy disk patterns located such that they are separated by the resolution limit. In order to detect this profile using a scientific camera, you would need a pixel at each peak and one at the minimum between the two peaks. The minimum is half way between the two peaks, leading to the requirement that your pixel size needs to be at least one half of the minimum resolution.

If your pixel size is smaller such that you have three or four pixels per resolution feature, then you will be oversampling and eliminate errors due to aliasing. Table 1 provides the resolution limit for various microscope objectives and how typical cameras relate from a sampling perspective due to their pixel size. The pixel sizes have been divided up into three sizes: small (3.5 µm), medium (6.5 µm), and large (14 µm). In terms of camera comparison, the small pixel would correspond most closely to scientific-grade CMOS, the medium pixel would match the closest to scientific-grade CMOS and CCD, and the large pixel would best represent EMCCD. The pink highlighted cells do not meet the minimum sampling requirements based on the Rayleigh criterion. Green highlighted cells oversample sufficiently to suppress errors due to aliasing.

By using a 0.5× coupler in tandem with the

Figure 3:
Aliasing of a brick wall by undersampling.
Credits: This picture was provided by Cburnett on Wikipedia (http://upload.wikimedia.org/wikipedia/commons/f/fb/Moire_pattern_of_bricks_small.jpg).

various objectives, it is possible to maintain a sufficient sampling frequency with smaller pixels while allowing a higher throughput of light. Table 2 provides the resolution limit comparison when using the various microscope objectives combined with a 0.5× coupler. The red highlighted cells do not meet the sampling requirements. Green highlighted cells oversample sufficiently to suppress errors due to aliasing.

Depth of Field
The depth of field (D_f) of a microscope is the distance that the sample can be shifted along the optical axis and still remain in focus. Conceptually, this corresponds to the distance that the sample can be defocused with the resulting blur remaining within the resolution limit defined in the previous section. The D_f is proportional to the index of the sample and the wavelength of light and it is inversely proportional to the square of the NA of the objective [3]:

$$D_f = 2n\lambda/NA^2 \qquad (4)$$

For most widefield microscopy, the fluorescent emission point sources of interest are within a portion of the depth of field. As such, other fluorescence signal not focused upon is considered background and not part of the true signal of interest. The equations described here are consistent with such use-case scenarios. For thicker samples, where a significant amount of fluorescence traverses the entire depth of field and confocal techniques must instead be employed, another analytical approach and a different set of equations should be utilized.

RADIOMETRIC ANALYSIS
A critical parameter for any imaging experiment is the signal-to-noise ratio (SNR). As the SNR of an image increases, the quality of the acquired image will also increase. As a first step in the determination of the SNR, this section of the article provides a methodology for estimating the expected signal in the form of photons detected by the sensor per pixel (Φ). Discussion of noise and SNR for the three camera technologies will be set forth in Part 3 of this series.

Optical Throughput
Figure 5 depicts a simple optical system as would be expected in the detection arm of a microscope. The source is emitting photons,

which are collected by the objective lens. The total number of photons emitted by the source and collected by the objective lens is described by Equation 5:

$$\Phi = L\, A_s\, \Omega_o \qquad (5)$$

where L is the radiance of the source; A_s is the area of the source; and Ω_o is the solid angle at the object. The solid angle describes the 3D cone into which light is emitted and collected by the objective lens. Equation 6 shows the relationship between solid angle and the NA of the objective lens:

$$\Omega_o = \pi\, NA^2 \qquad (6)$$

The product of the source area and the solid angle is known as the optical throughput. Based on geometrical considerations, it can be shown that the optical throughput (Λ) at the detector is equivalent to the optical through-put at the source, as shown in Figure 5 and Equation 7. The same analysis can be done at the pixel level of the sensor to calculate the expected signal at each pixel of the sensor (Φ_p).

Table 3 shows how the optical throughput changes with the parameters of the micro-scope objective. It is important to note that as the NA increases, the throughput increases. However, with commercially available objec-tive lenses, increases in NA are often accom-panied by increases in magnification, which reduces throughput:

$$\Lambda = A_s \Omega_o = A_d \Omega_i \qquad (7)$$

Detected Photons
The only unknown in Equation 5 is the radi-ance (L) of the fluorescent source. The radi-ance is defined as the photons emitted per sec-ond per unit area per unit solid angle [4]. Unlike a light source, where radiometric para-meters like lumens are measured and known, the radiance of the fluorescent sample has to be calculated based on other known parame-ters. In fluorescence microscopy, the sample is comprised of molecules which are emitting a certain number of photon counts per second per molecule (cpsm). This parameter of the flu-orescent sample is known as molecular bright-ness ϵ [5] which is a function of the absorption cross-section σ at the excitation wavelength, the quantum yield γ of the fluorophore, and the excitation intensity I. The product of the molecular brightness and the dye concentra-tion χ provides a metric on the number of photons emitted per second per unit area (assuming a thin sample). Dividing this value by the solid angle of emission gives an esti-mate on the radiance per unit volume. Each fluorescent molecule is emitting photons into a full spherical solid angle. The solid angle of a sphere is 4π. When we consider how many photons are being collected by the optical sys-tem, we must consider the solid angle of the objective lens, which is related to its NA. Bring-ing all this together, we can get an expression for the expected signal per pixel per second based on known parameters of the sample
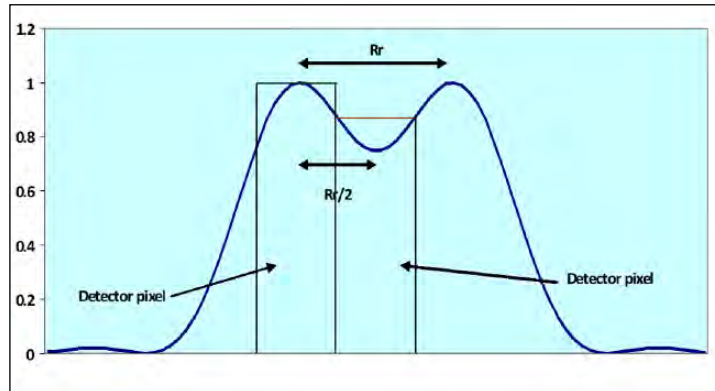

Figure 4:
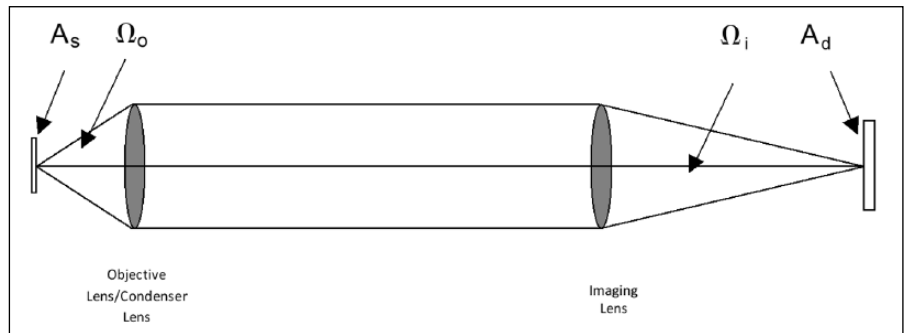Sampling requirement of two pixels per minimum resolution unit (Rayleigh criterion).

Figure 5:
Basic schematic of radiometric parameters in an optical imaging system.

Table 1: Sampling Factors For Different Cameras (< 2.0 is undersampled)							
MAG	Coupler	NA	Resolution Limit (@ sample in microns)	Resolution Limit (@ detector in microns)	3.5 micron pixel	6.5 micron pixel	14 micron pixel
10	1	0.45	0.75	7.46	2.13	1.15	0.53
20	1	0.75	0.45	8.95	2.56	1.38	0.64
40	1	0.95	0.35	14.13	4.04	2.17	1.01
40	1	1	0.34	13.42	3.83	2.06	0.96
40	1	1.3	0.26	10.32	2.95	1.59	0.74
60	1	1.2	0.28	16.78	4.79	2.58	1.20
60	1	1.3	0.26	15.48	4.42	2.38	1.11
100	1	1.4	0.24	23.96	6.85	3.69	1.71

Sufficient Sampling · Insufficient Sampling

Table 1:
Sampling factors for different cameras (<2.0 is undersampled).

Table 2: Sampling Factors For Different Cameras with 0.5x Coupler (< 2.0 is undersampled)							
MAG	Coupler	NA	Resolution Limit (@ sample in microns)	Resolution Limit (@ detector in microns)	3.5 micron pixel	6.5 micron pixel	14 micron pixel
10	0.5	0.45	0.75	3.73	1.07	0.57	0.27
20	0.5	0.75	0.45	4.47	1.28	0.69	0.32
40	0.5	0.95	0.35	7.06	2.02	1.09	0.50
40	0.5	1	0.34	6.71	1.92	1.03	0.48
40	0.5	1.3	0.26	5.16	1.47	0.79	0.37
60	0.5	1.2	0.28	8.39	2.40	1.29	0.60
60	0.5	1.3	0.26	7.74	2.21	1.19	0.55
100	0.5	1.4	0.24	11.98	3.42	1.84	0.86

Sufficient Sampling · Insufficient Sampling

Table 2:
Sampling factors for different cameras with 0.5X coupler (<2.0 is undersampled).

and the detection arm of the microscope:

$$\epsilon = \sigma(\lambda_{ex}) \, \gamma \, I_{ex} \qquad (8)$$

$$L = \epsilon \chi / 4\pi \qquad (9)$$

$$\Phi = L \, A_{s\,p} \, \Omega_o = \epsilon \chi \, NA^2 \, A_{d\,p} / (4 \, M^2) \quad (10)$$

Since this is an epi-fluorescence imaging system, we cannot forget that as the NA of the objective lens changes, the intensity of the excitation light incident on the sample will also change. Equation 10 shows that the detected number of photons changes as the square of the NA. Similarly, the incident number of photons and, hence, the molecular brightness will change as the square of the NA. Therefore, for epi-fluorescence systems, the number of photons reaching the sensor is ultimately proportional to the 4th power of the NA of the objective [6].

Table 4 shows the number of photons collected per pixel per second for typical pixel sizes of various commercially available sensors. The calculations assume a sample with a molecular brightness of 3300 cpsm (10× objective), having a concentration of 200 nM in the sample. Clearly, those sensors with larger pixels will trade off higher collection efficiency with lower resolution. Table 4 shows that, for a given magnification, increases in NA will lead to increases in photons collected because the solid angle is increasing both for illumination and detection. However, as the magnification of the objective increases, the total detected photons will not increase as quickly. This is the case because the increase in solid angle with increase in NA is offset by a reduction in the effective pixel area at the sample.

Table 5 shows how the detected photons per pixel increase when a 0.5× coupler is introduced into the detection arm. The critical point of Table 5 is that for the 3.5 μm pixel camera, a 0.5× coupler can be introduced to significantly increase the throughput while maintaining adequate sampling and not sacrificing resolution.

Further comparison of the 3.5 μm pixel camera using a 0.5× coupler with a 6.5 μm camera and no coupler shows that the 3.5 μm/0.5× coupler combination is preferable. Table 6 compares the two configurations for those four objectives where the sampling rate is sufficient to avoid aliasing. From this table, we can conclude that the 3.5 μm pixel camera with a 0.5× coupler will collect around 10% more light while maintaining adequate sampling. However, the addition of a coupler is not always desired as it can impart unwanted aberrations to the image reducing resolution. Alternatively, a high NA objective with a lower magnification could be used in conjunction with a small pixel camera to obtain a high signal level without under sampling. For example, using a 3.5 μm pixel camera with a 40× 1.3 NA objective would provide Nyquist sampling and comparable or even greater photons per pixel when the sample is detected with a 60× 1.3 NA objective using a 6.5 μm pixel sensor. Hence, using a 40× objective may be better than adding an optical element such as a

Table 3: Optical Throughput (Thin Sample)					
MAG	NA	Proj Solid Angle (ster)	3.5 micron pixel	6.5 micron pixel	14 micron pixel
10	0.45	0.636	0.078	0.269	1.247
20	0.75	1.767	0.054	0.187	0.866
40	0.95	2.835	0.022	0.075	0.347
40	1	3.142	0.024	0.083	0.385
40	1.3	5.309	0.041	0.140	0.650
60	1.2	4.524	0.015	0.053	0.246
60	1.3	5.309	0.018	0.062	0.289
100	1.4	6.158	0.008	0.026	0.121

Table 3:
Optical throughput (thin sample).

Table 4: Radiometric Parameters (No Coupler) - Detected Photons/Sec				
MAG	NA	3.5 micron pixel	6.5 micron pixel	14 micron pixel
10	0.45	62	214	993
20	0.75	120	413	1916
40	0.95	77	266	1233
40	1	95	326	1514
40	1.3	270	932	4325
60	1.2	87	301	1396
60	1.3	120	414	1922
100	1.4	58	201	931

Table 4:
Radiometric parameters (no coupler) - Detected photons per second.

Table 5: Radiometric Parameters (0.5X Coupler) - Detected Photons/Sec				
MAG	NA	3.5 micron pixel	6.5 micron pixel	14 micron pixel
10	0.45	231	797	3696
20	0.75	446	1537	7129
40	0.95	287	989	4588
40	1	352	1214	5633
40	1.3	1006	3468	16088
60	1.2	324	1119	5191
60	1.3	447	1541	7150
100	1.4	216	746	3462

Sufficient Sampling   Insufficient Sampling

Table 5:
Radiometric parameters (0.5X coupler) - Detected photons per second.

coupler into the optical path.

CONCLUSIONS

This article develops a methodology for understanding the balance between image resolution, sampling and optimal light throughput in microscopy systems where digital imaging technologies (CCD, EMCCD, and scientific-grade CMOS) are utilized.

Realistic experimental conditions, such as molecular brightness, dye concentrations, NA, and magnification, were used to compare Nyquist sampling and light throughput for the three camera technologies at different pixel sizes. The comparison showed that while smaller pixel cameras were able to provide better sampling at low magnifications, they were also less efficient at collecting light than the medium pixel scientific-grade CMOS and CCDs and the larger pixel EMCCDs.

Use of a 0.5× coupler was shown to increase the signal in smaller pixel cameras while still maintaining adequate sampling. However, the addition of another optical element in the detection arm is not always desirable because of additional light loss and the introduction of optical aberrations reducing resolution. Another exciting possibility, which uses a small pixel size camera with a lower magnification, high NA objective to improve light collection while adequately sampling, has also been proposed.

The next article in this series will discuss noise sources in digital imaging technologies and compare and contrast them for CCD, scientific-grade CMOS, and EMCCD cameras specifically.

| | | **Table 6: 6.5micron pixel vs 3.5micron pixel with 0.5X Coupler** | | | |
| | | 6.5 micron pixel - No Coupler | | 3.5 micron pixel - 0.5X Coupler | |
MAG	NA	Resolution Limit (@ detector in microns)	Detected Photons/Sec	Resolution Limit (@ detector in microns)	Detected Photons/Sec
40	0.95	14.13	266	7.06	287
60	1.2	16.78	301	8.39	324
60	1.3	15.48	414	7.74	447
100	1.4	23.96	201	11.98	216

Table 6:
6.5 µm pixel versus 3.5 µm pixel with 0.5X coupler.

REFERENCES

1. Sabharwal, Y. Digital Camera Technologies for Scientific Bio-Imaging. Part 1: The Sensors. Microscopy and Analysis 25(4):S5-S8 (AM), 2011.
2. www.microscopyu.com/articles/superresolution/diffractionbarrier.html
3. www.olympusmicro.com/primer/anatomy/objectives.html
4. http://micro.magnet.fsu.edu/primer/anatomy/imagebrightness.html
5. Muller, J. D. Cumulant analysis in fluorescence fluctuation spectroscopy. Biophys. J. 86:3981–3992, 2004.
6. http://zeiss-campus.magnet.fsu.edu/articles/lightsources/lightsourcefundamentals.html